Egyptian Geophysical Society
EGS Journal, vol. 6, No. 1, 81-101 (2008)

RESERVOIR QUALITY DISCRIMINATION OF THE LOWER PART OF BAHARIYA FORMATION IN NORTH QARUN OIL FIELD, WESTERN DESERT, EGYPT

A.A.A. Othman*, B.S. Nabawy**, T.H. Abdel Hafeez*,

M. Saher*** and R.R. AbdelKader****

** Department of Geology, Faculty of Science, AlAzhar University, Cairo.*
*** Department of Geophysical Sciences, National Research Centre, Cairo*
**** Apache Oil Company, Cairo*
***** North Bahariya Oil Company, Cairo*

تقدير الجودة الخزانية لصخور الجزء السفلى من مكون البحرية بحقل شمال قارون – الصحراء الغربية – مصر

الخلاصـة: تعتمد قيم الكثافة النوعية للجزء السفلى لمكون البحرية فى حقل شمال قارون على قيم المسامية المقدرة باستخدام غاز الهليوم أكثر من اعتمادها على كثافة الحبيبات كنتيجة لعدم تجانس التركيب المعدنى للعينات الاسطوانية المدروسة فى هذا الحقل. كما تعتمد قيم النفاذية المقاسة فى الاتجاهين العمودى والموازى للطبقات على المساميه المقاسة باستخدام غاز الهليوم اعتماداً كبيراً بينما تعتمد بدرجة أقل على قيم النفاذية المقاسة بطريقة مجموع السوائل المتبقية، حيث يمكن إعزاء ذلك لوجود محتوى طفلى عالى.

وتشير التحليلات الاحصائية لبيانات تحليل العينات الاسطوانية إلى تميز الجزء السفلى من مكون البحرية فى هذا الحقل بصفات خزانية جيدة (قيم مسامية ونفاذية عالية وقيم كثافة كلية وعدم تجانس قليل لقيم النفاذية). وعلى الجانب الآخر تصل القيم المقاسة لعدم التجانس فى النطاقات غير الخزانية إلى ٣٥ مما يعطى درجة عالية من عدم التجانس فى توزيع الصفات الخزانية فى الاتجاهات الثلاثة مما يعنى درجة أعلى لالتوائية المسارات الفراغية وتعقيدها. ويمكن إعزاء ذلك إلى التأثير العشوائى لعمليات التغير اللاحقة والمؤثرة على النطاقات المدروسة فى الحقل. كما يلاحظ وجود قيم لعدم التجانس أقل من الواحد الصحيح مما يعنى قيم أعلى للنفاذية المقاسة فى الاتجاه الرأسي عن مثيلاتها فى الاتجاه الأفقى مما يوحى بوجود نفاذية ومسامية ناتجة عن شروخ مؤثرة رأسياً فى الخزان. وينصح باستخدام هذه القيم العالية لعدم التجانس فى عمليات المقارنة بين الأبار المختلفة وتتبع الطبقات خلالها.

وبتطبيق طريقة أمافول يمكن بدرجه عالية تمييز النطاقات عالية التخزين والمميزة داخل الخزان، حيث وجد تطابق جيد بين قيم كفاءة الخزان والقيم المسجلة لنطاقات التدفق داخل الخزان.

ABSTRACT: *The horizontal and vertical permeability values (kH and kV) are dependant mainly upon the measured porosity in a very good direct proportional relationship. Helium porosity values are more precious than the summation fluids porosity for calculating permeability in both vertical and horizontal permeability due to the high clay content.*
The statistical analysis of the core data showed good storage capacity properties through the middle and upper parts of the studied sections of Bahariya Formation in N. Qarun Oil Field. It is characterized by high porosity, high permeability, low bulk density and low anisotropy values (< 2.14). The anisotropy values of the other bad storage capacity horizons, may reach up to 35 which gave rise to heterogeneity in the storage capacity distribution in the 3D, more channel and pore throat complexity. This could be attributed to a random effect of the diagenetic factors through the studied depth interval. Presence of some anisotropy fraction values (< 1.0) is attributed mainly to vertical fracture permeability has acted through the vertical plain, whereas presence of very high anisotropy values (up to 35) could be attributed to some fissile beds containing high clay content. However, these anisotropy anomalies are recommended to be used as marker anomalies or traces to follow up the bay zones through the different bore holes.
Application of the technique of Amaefule et al. (1993) allows a more precise definition of reservoir discrimination. Excellent agreement was obtained between the vertical distribution of Reservoir Quality Index (RQI) and Flow Zone Indicator (FZI).

INTRODUCTION

The North Western Desert has simple monotonous geological surface features and complicated subsurface successions. The sedimentary sequence in this area has been studied and dated by several authors, e.g. Kostandi (1959), Said (1962), El Gezeery et al. (1972), Barakat and Darwish (1987), Hanter (1990), Ibrahim (2002), Lüning et al. (2004) etc.

Generally, thickness of the sedimentary section increases northward reflecting different basins throughout the geologic history of the unstable shelf. Drilling activities have revealed that the sedimentary sequence is thick and ranges in age from Paleozoic up to Tertiary and also have identified many sedimentary basins of different ages. All these basins are characterized by having not only oil/gas generating source rocks but also the presence of the reservoir rocks with appreciable storage capacity regarding porosity and permeability values.

Shifting of depocenteres in a consistently subsiding area such as the north Western Desert has produced a wide range of sedimentary environments, many of which provide favourable conditions for hydrocarbon generation and entrapment (Schlumberger; 1984). Moreover, the structural controls of the northern part of the Western Desert play an important role in the configuration of these rocks as reservoirs.

The North Qarun Oil field area is restricted between latitudes 29° 46′ & 29° 49′ N and longitudes 30° 33′ & 30° 35′ E with total surface area of about 5 km^2 (Fig. 1).

It is bounded by Wadi El Natrun to the North, Qarun Lake and Wadi El Raiyan to the south, the Qattara Depression to the west and the River Nile to the east. The study area is covered mainly by the Lower Miocene "Moghra Formation" (Tammam, 1996).

The subsurface studies and investigations of the North Western Desert such as aeromagnetic measurements, gravity, seismic and drilling revealed the following subsurface stratigraphic column from Paleozoic to Recent (Fig. 2).

The subsurface Cretaceous rocks, in particular, have attracted the attention of many workers, where they are widely distributed and represent a major target for oil exploration.

The present study analyzes and focuses on the storage capacity properties and reservoir quality discrimination of the lower part of Bahariya Formation of the North Qarun Oil Field, and distinct the anisotropy of the permeability distribution in directions perpendicular and parallel to the bedding plane.

The reservoir quality discrimination was carried out by using the technique published by Amaefule et al. (1993) which allows a more precise definition of reservoir discrimination through a combination of the permeability and porosity data.

SUBSURFACE STRATIGRAPHY

The Late Cretaceous time in Egypt could be assigned by a major marine transgression resulted in the deposition of a dominantly carbonate thick sequence (Said, 1962). The Upper Cretaceous sediments are subdivided into three rock formations; Bahariya Formation, Abu Roash Formation and Khoman Formation.

The Bahariya Formation, the scope of the present study, was firstly assigned by (Said, 1964) to describe a Lower Cenomanian fluvio-marine conditions prevailed by the begging of the Late Cretaceous time. During this time, argillaceous sandstone sequence intercalated with some carbonates interbeds was deposited.

Abdalla and El-Bassyouni (1985) proposed that, this formation was deposited firstly in dominant fluviatile conditions, followed by estuarine conditions and finally lagoonal conditions prevailed. The Bahariya sandstones show good oil and gas production in the Alamein and Abu Gharadig Oil Fields.

It is also the main producing horizon in the Razzak, Aghar, Ahram, Meleiha, Salam, and Neag Oil Fields (Schlumberger, 1984). The Isopach contour map of Bahariya Formation shows an erratic distribution pattern with a maximum thickness reaches up to 400 ft recorded at Qattara 1-x well (Fig. 3). On the other side, Bahariya Formation is occasionally thin or completely disappears giving a place to the overlying Abu Roash "G" Member.

From the stratigraphic point of view, Qarun concession can be subdivided into three stratigraphic provinces, they are the Kattaniya province (North West of Qarun), El Sagha province and Wadi El Raiyan province (South of Qarun) as shown in figure 4 (Abd El Aal and Moustafa, 1988).

Most of the oil discoveries in the Qarun concession are located at the northern and southern flanks of El Gindi basin, namely El Sagha and Wadi El Raiyan provinces, only the WD19 Oil Field is located in the Kattaniya inverted basin (Abd El Aal and Moustafa, 1988).

STRUCTURAL FEATURES AND OUTLINES OF QARUN OIL FIELD

The structures of the Qarun concession and the surrounded area are mainly related to a Jurassic/Early Cretaceous extensional phase followed by the Cretaceous/Eocene phase of inversion. These two phases of deformation are related to the movements between the African and Eurasian plates. They include both folding and faulting processes; folds in El Sagha trend are oriented NE-SW as asymmetrical folds with steep northwestern flanks and gentle southeastern flanks. On the other hand, the faults of the Qarun concession have three main orientations, ENE-WSW, NE-SW and NW-SE (Abd El Aal and Moustafa, 1988, Abdel El Aal, 1990), could be described as follows:

1) **ENE -WSW** oriented faults, dominated in the northern and southern most parts of Qarun concession. These faults have an apparent normal slip.

2) **NE-SW** oriented faults, common in the El Sagha province and represented by steep southeast dipping reverse faults bounding the northern flanks of the folds of the El Sagha province.

3) **NW-SE** oriented faults, predominantly normal and active for at least two times: (a) at the Early to Late Cretaceous time, causing increase in thickness of the Lower Cretaceous sequence as well as Abu Roash Formation on the down thrown sides of these faults, and (b) at times following the extrusion of the Lower Miocene basalt flows in the North Western Desert.

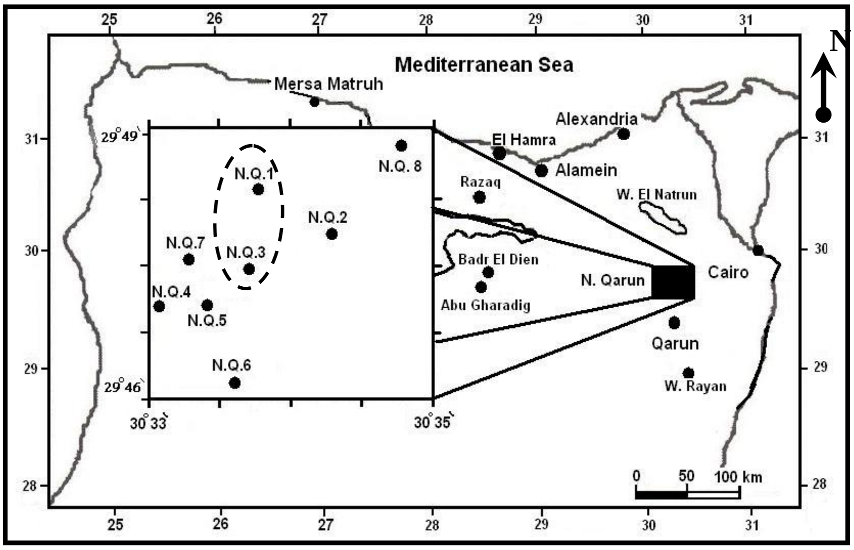

Fig. (1) Location Map of the Studied wells in North Qarun Oil Field.

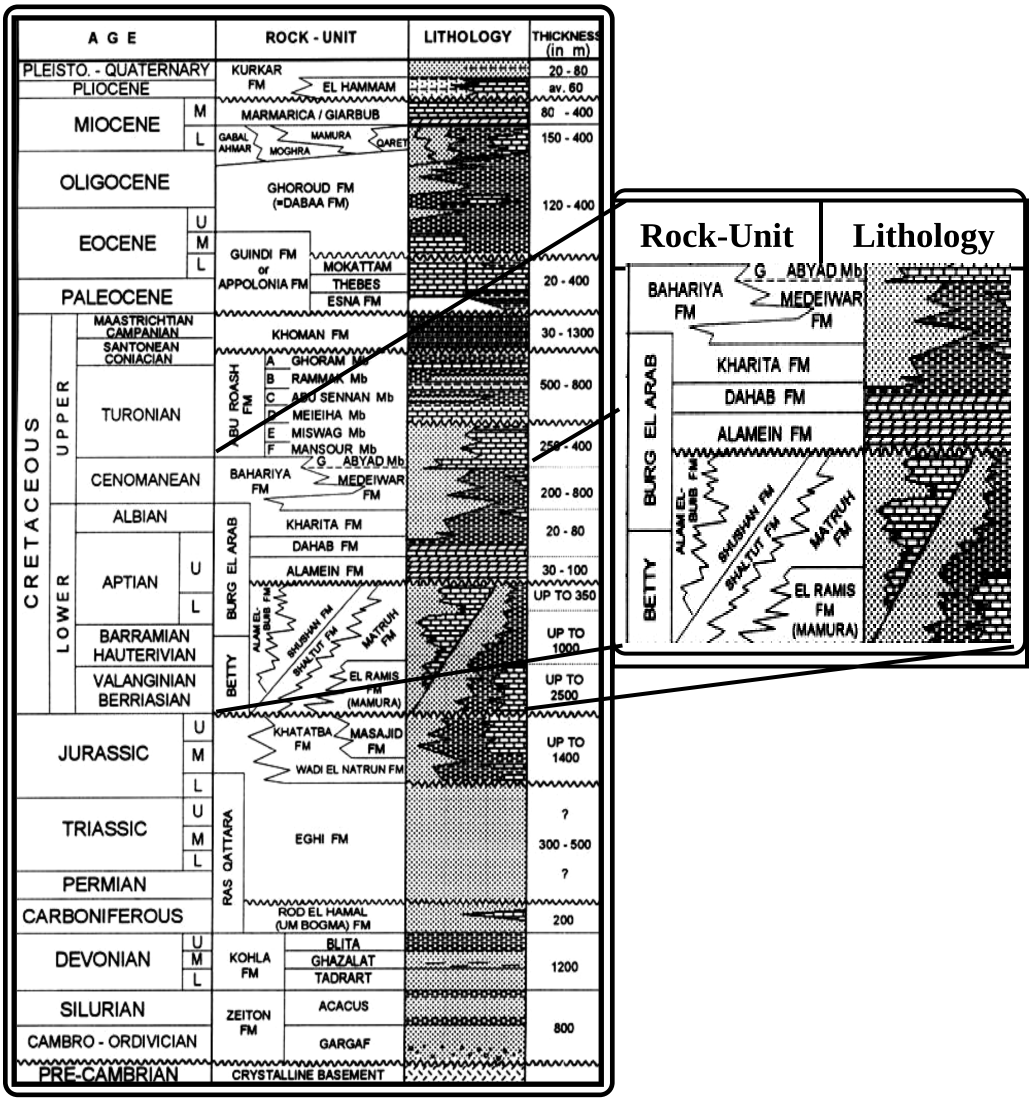

Fig. (2) A Composite Lithostratigraphic Column of the Northern Part of the Western Desert (Schlumberger; 1984 & 1995).

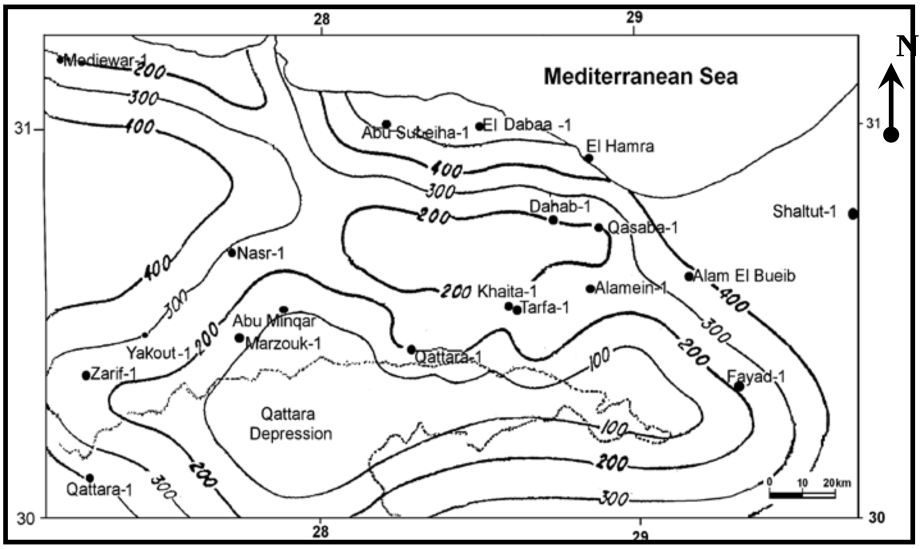

Fig. (3) Isopach Contour Map of Bahariya Formation, North Western Desert (El Shaarawy, 1994), C.I = 100 ft.

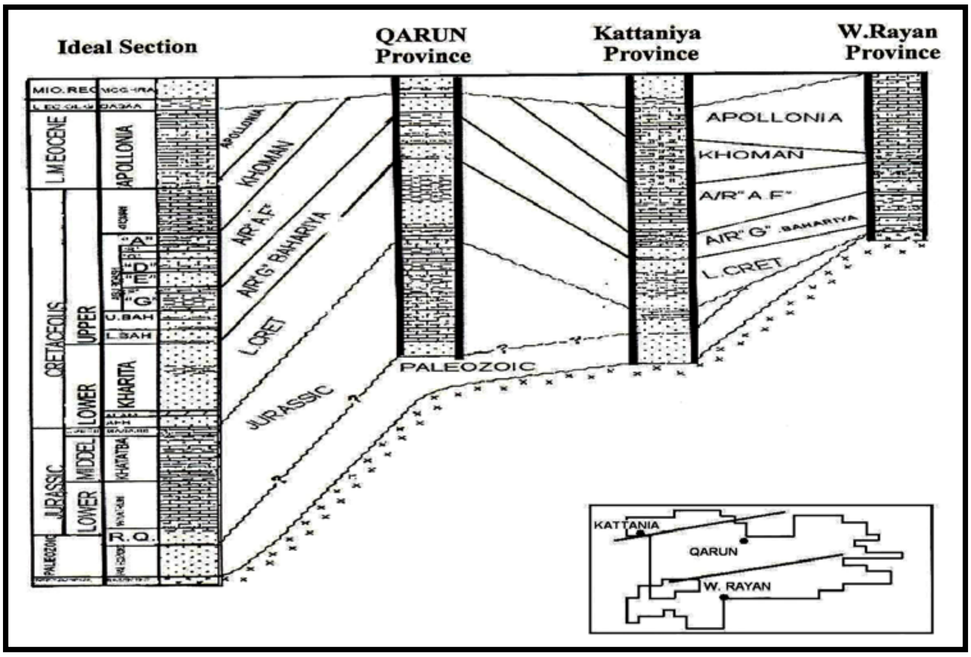

Fig. (4) Stratigraphy of the Main Provinces in the Qarun Concession (Abd El-Aziz et al., 1998).

The depth map of North Qarun Oil Field at the lower Bahariya level shows a fault structure, bounded at its southwestern part by a major NW-SE trending normal faulting and at the northwestern side by NE-SW strike slip faults belonging to the Syrian Arc System (Fig. 5).

THEORETICAL BACKGROUND

The reservoir quality index (RQI) is defined as the square root of the ratio between permeability and porosity (Amaefule et al., 1993). This term can be used to qualify the flow character of a reservoir and provide a good relationship between petrophysical properties at micro level (core plug) and macro levels (well bore).

The use of the approach of Amaefule et al. (1993) allows for a more quantitative reservoir zonation. This method has been used in the classification of the reservoir rock quality for characterization of carbonate reservoirs. It was tested and successfully applied by many authors to qualify the reservoir quality, e.g. Tiab and Donaldson, 1996; El-Sayed et al., 2005; Al-Dhafeeri and Nasr-El-Din, 2007; etc

The calculation of the Reservoir Quality Index (RQI) in µm, and the Normalized Porosity Index (NPI) in volume fraction, are based on the following equations (Amaefule et al., 1993):

$$RQI = 0.0314\sqrt{\frac{k}{\varnothing}}$$ (Amaefule et al., 1993) (1)

where

k Permeability, md

∅ Porosity, volume fraction

And NPI is expressed as:

$$NPI = \frac{1-\varnothing}{\varnothing}$$ (Amaefule et al., 1993) (2)

RQI and NPI are then used to determine the Flow Zone Indicator (FZI), which is used to qualify the flow character of the aquifer/reservoir. FZI is expressed as follows:

$$FZI = \frac{RQI}{NPI} = \frac{0.0314\sqrt{k/\varnothing}}{\varnothing/(1-\varnothing)}$$ (Amaefule et al., 1993) (3)

To reveal the anisotropy of permeability measured by applying the vertical (k_V) and horizontal values (k_H), a scale of anisotropy of permeability (γ) is defined here as:

$$\gamma = \sqrt{\frac{k_H}{k_V}} \quad (4)$$

MEASURED DATA

A routine core analysis including nitrogen permeability determination horizontally and vertically, helium porosity, and summation fluids porosity has been conducted for 249 core samples by Corex for the order of Qarun Petroleum Company. The analysis was limited to two representative bore holes, N. Qarun-1 and N. Qarun-3 (Fig. 1). The core analysis has been conducted for a total of 110 core samples representatively elected from the lower part of Bahariya Formation in well N. Qarun-1 (Table 1), and 139 core samples from well N. Qarun-3 (Table 2).

The studied samples of the lower part of Bahariya Formation in both wells are mostly composed of light grey, fine to very fine and well sorted sandstones, slightly cemented by siliceous cement. A negligible amount of pyrite and glauconite content are sometimes noticed.

The determined bulk density values of were found to vary from 2.14 to 2.63 g/cm^3 with average 2.31 g/cm^3 for N. Qarun-1 samples whereas N. Qarun-3 samples have bulk density values varying in between 2.12 and 3.05 with average 2.35 g/cm^3. The grain density values of N. Qarun-1, on the other side, vary from 2.65 to 2.82 g/cm^3 with average 2.68 g/cm^3, whereas for N. Qarun-3 samples, it varies from 2.63 to 3.25 g/cm^3 with average 2.69 g/cm^3 (Tables 1 and 2). The relatively high density of some N. Qarun-3 samples could be attributed to some iron oxides and heavy mineral contents. The bulk density values are displayed as functions in depth (in feet) in figures 16 and 17.

The Helium porosity values for N. Qarun-1 samples vary from 2.4 up to 19.7 % with average 13.1 % and for N. Qarun-3 samples vary from 1.2 up to 20.4 % with average 12.3 %. The Helium porosity values are also displayed as functions in depth in figures 16 and 17. The fluid summation porosity varies from 3.6 up to 22.3 % with average 13.1 % for N. Qarun-1 samples and from 2.5 up to 22.1 % of mean equals 11.9 % for N. Qarun-3 samples (Tables 1 and 2).

On the other hand, the measured nitrogen permeability in the horizontal direction vary from 0.01 to 937 mD (of average 148.01 mD), and from 0.01 to 1844 mD (of average 168.2 mD) for samples from wells N. Qarun-1 and N. Qarun-3, respectively; whereas the vertical permeability varies from 0.02 to 924 mD (of average 92.4 mD) and from 0.01 to 1244 mD (of average 103.3 mD) for samples from wells N. Qarun-1 and N. Qarun-3, respectively. The nitrogen permeability values are plotted against depth in figures 16 and 17.

POROSITY, PERMEABILITY AND DENSITY INTERRELATIONSHIPS

The determined bulk density values for samples from N. Qarun-1 well, are mostly dependant on the Helium porosity values rather than the dependence on the grain density values (Fig. 6, r = - 0.98 and r = 0.73, respectively) due to a more or less heterogeneity in the mineralogical composition of the studied samples.

Table 1. Porosity, Permeability, Density, Anisotropy of Permeability, Reservoir Quality Index (RQI) and Flow Zone Indicator (FZI) Data for the Sampled Rocks from the Lower Part of Bahariya Formation, Well N. Qarun-1, N. Qarun Oil Field, Western Desert, Egypt.

Depth	Helium Porosity	Summation Fluids Porosity	Bulk Density	Grain Density	Nitrogen Permeability		Anisotropy	Reservoir Quality Index	Flow Zone Indicator
					Horizontal	Vertical			
8869	8.00	17.00	2.48	2.70	12.20	0.06	14.26	0.39	4.46
8871	10.60	8.10	2.43	2.72	3.73	0.05	8.64	0.19	1.57
8873	8.70	7.60	2.44	2.67	10.10	0.09	10.59	0.34	3.55
8874	10.50	8.60	2.42	2.70	2.83	0.83	1.85	0.16	1.39
8879	15.20	12.10	2.49	2.73	0.06	0.04	1.22	0.02	0.11
8880	14.20	14.80	2.42	2.69	0.13	0.06	1.47	0.03	0.18
8881	7.70	5.30	2.51	2.70	6.02	0.03	14.17	0.28	3.33
8882	12.40	9.10	2.60	2.70	0.13	0.10	1.14	0.03	0.23
8883	10.00	11.80	2.45	2.69	0.36	0.05	2.68	0.06	0.54
8888	7.80	7.20	2.35	2.72	1.65	0.06	5.24	0.14	1.71
8892	6.60	4.80	2.40	2.78	0.22	0.03	2.71	0.06	0.81
8893	4.80	3.60	2.25	2.69	3.40	0.05	8.25	0.26	5.24
8894	7.70	5.60	2.21	2.65	1.32	0.23	2.40	0.13	1.56
8896	2.40	8.80	2.18	2.74	0.01	0.02	0.71	0.02	0.82
8897	11.80	10.20	2.29	2.66	37.70	28.70	1.15	0.56	4.20
8898	9.80	15.30	2.19	2.66	2.06	1.60	1.13	0.14	1.33
8899	15.80	15.30	2.16	2.67	27.20	46.00	0.77	0.41	2.20
8900	17.20	15.10	2.23	2.67	310.0	236.0	1.15	1.33	6.42
8901	18.40	15.90	2.30	2.67	437.0	346.0	1.12	1.53	6.79
8902	14.70	20.90	2.27	2.69	38.70	17.70	1.48	0.51	2.96
8903	17.90	19.10	2.14	2.67	261.0	140.0	1.37	1.20	5.50
8904	18.80	22.00	2.23	2.66	435.0	317.0	1.17	1.51	6.52
8907	17.00	18.60	2.24	2.69	33.20	21.60	1.24	0.44	2.14
8908	14.60	16.50	2.24	2.69	40.70	37.40	1.04	0.52	3.07
8909	15.10	16.50	2.28	2.67	51.70	94.80	0.74	0.58	3.27
8910	19.70	22.30	2.40	2.67	55.90	360.0	0.39	0.53	2.16
8911	16.80	19.50	2.38	2.68	208.0	41.10	2.25	1.10	5.47
8913	17.40	19.60	2.41	2.71	31.30	14.80	1.45	0.42	2.00
8914	16.60	17.90	2.40	2.69	25.00	58.40	0.65	0.39	1.94
8915	16.00	18.10	2.46	2.72	42.50	30.80	1.17	0.51	2.69
8916	10.00	11.30	2.34	2.67	1.64	0.66	1.58	0.13	1.14
8917	11.50	9.70	2.24	2.69	16.20	4.35	1.93	0.37	2.87
8918	9.30	9.20	2.35	2.66	3.10	0.99	1.77	0.18	1.77
8919	10.00	12.50	2.34	2.67	2.87	1.18	1.56	0.17	1.51
8920	7.70	13.50	2.51	2.67	2.23	3.88	0.76	0.17	2.03
8921	12.20	9.20	2.34	2.67	18.60	12.00	1.24	0.39	2.79
8922	15.80	16.60	2.32	2.66	178.0	113.0	1.26	1.05	5.62
8923	12.30	9.80	2.37	2.68	2.40	1.07	1.50	0.14	0.99
8924	12.50	11.40	2.34	2.67	16.60	10.20	1.28	0.36	2.53
8925	7.70	4.70	2.31	2.72	0.84	0.05	4.10	0.10	1.24
8926	12.20	7.50	2.30	2.67	30.10	12.50	1.55	0.49	3.55
8929	13.90	8.20	2.25	2.69	60.90	14.70	2.04	0.66	4.07
8930	11.30	9.70	2.27	2.67	13.10	6.67	1.40	0.34	2.65
8931	12.40	13.50	2.23	2.67	42.10	26.60	1.26	0.58	4.09
8932	13.00	13.50	2.26	2.66	111.0	79.30	1.18	0.92	6.14
8933	14.00	9.80	2.25	2.67	114.0	12.40	3.03	0.90	5.50
8934	15.40	20.00	2.34	2.66	134.0	53.10	1.59	0.93	5.09
8937	15.00	10.60	2.25	2.67	163.0	129.0	1.12	1.04	5.87
8938	16.00	15.10	2.34	2.66	657.0	256.0	1.60	2.01	10.56
8939	15.30	13.40	2.17	2.67	136.0	170.0	0.89	0.94	5.18
8940	15.60	15.80	2.18	2.66	172.0	95.10	1.34	1.04	5.64
8941	12.10	15.10	2.19	2.66	21.00	5.28	1.99	0.41	3.01

Table 1. Continued.

Depth	Helium Porosity	Summation Fluids Porosity	Bulk Density	Grain Density	Nitrogen Permeability		Anisotropy	Reservoir Quality Index	Flow Zone Indicator
					Horizontal	Vertical			
8942	15.90	14.40	2.28	2.67	113.00	30.90	1.91	0.84	4.43
8943	11.90	16.00	2.18	2.66	31.70	5.49	2.40	0.51	3.79
8944	18.40	15.20	2.25	2.66	452.0	225.0	1.42	1.56	6.90
8945	18.00	16.90	2.15	2.66	506.0	55.30	3.02	1.66	7.58
8946	17.50	13.80	2.20	2.66	382.0	153.0	1.58	1.47	6.92
8947	14.20	8.70	2.23	2.66	441.0	382.0	1.07	1.75	10.57
8948	18.20	15.80	2.17	2.66	775.0	924.0	0.92	2.05	9.21
8949	15.60	9.80	2.16	2.66	391.0	82.80	2.17	1.57	8.50
8950	19.30	16.80	2.17	2.66	648.0	106.0	2.47	1.82	7.61
8951	17.20	13.60	2.22	2.66	937.0	190.0	2.22	2.32	11.16
8952	16.50	14.40	2.23	2.67	337.0	171.0	1.40	1.42	7.18
8953	18.30	11.90	2.26	2.66	838.0	260.0	1.80	2.12	9.49
8954	19.10	16.70	2.21	2.67	293.0	70.50	2.04	1.23	5.21
8955	18.30	15.60	2.19	2.66	411.0	213.0	1.39	1.49	6.64
8956	16.40	16.60	2.19	2.66	655.0	451.0	1.21	1.98	10.12
8957	16.00	16.70	2.23	2.66	569.0	385.0	1.22	1.87	9.83
8958	15.20	16.30	2.15	2.66	70.60	19.80	1.89	0.68	3.78
8959	17.30	16.10	2.22	2.67	152.0	69.60	1.48	0.93	4.45
8960	17.70	12.80	2.20	2.66	224.0	137.0	1.28	1.12	5.19
8961	18.00	20.90	2.21	2.67	549.0	385.0	1.19	1.73	7.90
8962	16.10	17.80	2.14	2.66	183.0	102.0	1.34	1.06	5.52
8963	19.20	15.50	2.44	2.66	450.0	317.0	1.19	1.52	6.40
8964	16.70	18.70	2.68	2.67	173.0	71.70	1.55	1.01	5.04
8965	17.40	18.40	2.41	2.66	252.0	228.0	1.05	1.19	5.67
8966	17.20	18.60	2.37	2.67	279.0	215.0	1.14	1.26	6.09
8967	19.40	18.20	2.37	2.66	592.0	205.0	1.70	1.73	7.21
8968	9.50	5.10	2.35	2.70	2.39	0.04	7.73	0.16	1.50
8969	4.80	10.00	2.40	2.82	0.15	0.02	2.74	0.06	1.10
8970	10.20	8.10	2.49	2.68	0.19	0.06	1.78	0.04	0.38
8971	14.70	6.30	2.46	2.69	0.12	0.14	0.93	0.03	0.16
8972	14.70	7.00	2.43	2.69	0.12	0.10	1.10	0.03	0.16
8973	12.20	10.90	2.40	2.69	0.07	0.05	1.18	0.02	0.17
8974	14.50	14.30	2.40	2.68	0.19	0.07	1.65	0.04	0.21
8975	12.60	4.70	2.35	2.69	0.17	0.06	1.68	0.04	0.25
8976	11.30	8.70	2.40	2.67	0.28	0.11	1.60	0.05	0.39
8977	11.40	3.60	2.36	2.68	0.16	0.10	1.26	0.04	0.29
8978	12.30	6.30	2.34	2.68	0.31	0.08	1.97	0.05	0.36
8979	10.40	6.60	2.36	2.68	0.24	0.10	1.55	0.05	0.41
8980	7.40	6.40	2.37	2.69	0.19	0.09	1.45	0.05	0.63
8981	8.40	13.30	2.32	2.69	0.68	0.05	3.69	0.09	0.97
8982	9.30	10.80	2.29	2.68	0.12	0.07	1.31	0.04	0.35
8983	10.60	9.10	2.67	2.69	0.28	0.09	1.76	0.05	0.43
8984	11.00	8.00	2.29	2.70	0.31	0.08	1.97	0.05	0.43
8985	12.60	12.10	2.36	2.69	0.47	0.82	0.76	0.06	0.42
8986	11.10	10.00	2.35	2.70	0.40	0.08	2.24	0.06	0.48
8987	12.30	12.50	2.31	2.69	2.91	4.57	0.80	0.15	1.09
8988	12.50	13.20	2.56	2.67	51.20	12.30	2.04	0.64	4.45
8989	11.40	9.50	2.29	2.66	60.00	41.00	1.21	0.72	5.60
Mean	13.50	12.70	2.31	2.68	148.01	83.17	2.14	0.73	3.95
Min	2.40	3.60	2.14	2.65	0.01	0.02	0.39	0.02	0.11
Max	19.70	22.30	2.68	2.82	937.0	924.0	14.26	2.32	11.16

Table 2. Porosity, Permeability, Density, Anisotropy of Permeability, Reservoir Quality Index (RQI) and Flow Zone Indicator (FZI) Data for the Sampled Rocks from the Lower Part of Bahariya Formation, Well N. Qarun-3, N. Qarun Oil Field, Western Desert, Egypt.

Depth	Helium Porosity	Summation Fluids Porosity	Bulk Density	Grain Density	Nitrogen Permeability		Anisotropy	Reservoir Quality Index	Flow Zone Indicator
					Horizontal	Vertical			
8787	2.8	5.1	2.69	2.77	0.08	0.03	1.63	0.05	1.84
8788	15.1	13.7	2.30	2.71	94.1	26.1	1.90	0.78	4.41
8789	20.4	14.6	2.13	2.67	627	516	1.10	1.74	6.79
8790	14.1	16.6	2.28	2.65	82.9	60.6	1.17	0.76	4.64
8791	17.2	12.9	2.21	2.67	289	171	1.30	1.29	6.20
8792	12.6	14.9	2.32	2.65	45	23.2	1.39	0.59	4.12
8793	9.2	11.7	2.43	2.68	0.17	0.02	2.92	0.04	0.42
8795	14	15.8	2.29	2.66	24.3	9.17	1.63	0.41	2.54
8796	18.1	19.8	2.19	2.67	184	114	1.27	1.00	4.53
8797	18.1	19.7	2.18	2.66	390	296	1.15	1.46	6.60
8798	18.2	19.1	2.18	2.67	220	219	1.00	1.09	4.91
8799	15.6	13	2.25	2.67	69.9	19.7	1.88	0.66	3.60
8800	15.5	16.2	2.25	2.66	52.9	12.2	2.08	0.58	3.16
8801	14.3	15.2	2.28	2.66	17.9	5.43	1.82	0.35	2.11
8802	13	11.6	2.31	2.66	26.7	0.31	9.28	0.45	3.01
8803	11	15.2	2.37	2.66	9.1	18.7	0.70	0.29	2.31
8804	12.9	10.5	2.34	2.69	17.9	7.47	1.55	0.37	2.50
8806	6.4	10.4	2.51	2.68	0.16	0.13	1.11	0.05	0.73
8825	10.7	11	2.38	2.66	28.6	40.3	0.84	0.51	4.28
8826	10	12.2	2.41	2.68	16.7	1.51	3.33	0.41	3.65
8828	4.8	6.5	2.59	2.72	58.4	0.04	38.21	1.10	21.72
8829	17.1	18.1	2.21	2.66	323	50.9	2.52	1.36	6.62
8830	14.4	10.6	2.28	2.66	76.7	65	1.09	0.72	4.31
8831	15.2	16	2.27	2.68	104	37.1	1.67	0.82	4.58
8832	8.2	14.3	2.45	2.67	1.17	0.38	1.75	0.12	1.33
8833	17.3	14.9	2.20	2.66	179	149	1.10	1.01	4.83
8834	14.1	16.6	2.28	2.65	62	50.4	1.11	0.66	4.01
8835	14.1	12.1	2.28	2.66	62	7.72	2.83	0.66	4.01
8836	19.3	18.4	2.15	2.67	504	234	1.47	1.60	6.71
8837	14.3	15.4	2.29	2.67	105	22.4	2.17	0.85	5.10
8838	19	22.1	2.15	2.65	553	386	1.20	1.69	7.22
8839	10.8	14.5	2.37	2.66	7.25	1.06	2.62	0.26	2.12
8840	15.1	14.1	2.27	2.67	137	22.9	2.45	0.95	5.32
8842	10.5	14.6	2.38	2.66	8.76	26.7	0.57	0.29	2.44
8843	10	11.7	2.40	2.67	4.89	0.94	2.28	0.22	1.98
8844	3.6	6.4	2.56	2.66	2.95	0.18	4.05	0.28	7.61
8846	9.5	10.1	2.40	2.65	12	3.29	1.91	0.35	3.36
8847	9.4	6.8	2.41	2.66	3.27	8.99	0.60	0.19	1.79
8848	8.9	11.0	2.44	2.68	8.5	0.56	3.90	0.31	3.14
8849	11.3	13.4	2.38	2.68	6.81	17.7	0.62	0.24	1.91
8850	14.5	13.7	2.27	2.66	150	42.2	1.89	1.01	5.96
8851	14	13	2.29	2.66	139	12.8	3.30	0.99	6.08
8853	15.8	16.8	2.24	2.66	234	91.7	1.60	1.21	6.44
8854	14.5	10.6	2.27	2.66	149	80.5	1.36	1.01	5.94
8855	14.5	11.7	2.29	2.68	94.6	5.24	4.25	0.80	4.73
8856	14	10.2	2.29	2.66	299	3.4	9.38	1.45	8.91
8857	12.8	9.1	2.32	2.66	58.5	8.47	2.63	0.67	4.57
8858	12.2	16.4	2.34	2.67	28.5	15.9	1.34	0.48	3.45
8859	15.9	13.3	2.24	2.66	209	43.3	2.20	1.14	6.02
8860	17.4	15.7	2.21	2.67	389	283	1.17	1.48	7.05
8861	17.4	19	2.21	2.67	542	577	0.97	1.75	8.32
8862	17.4	16.4	2.20	2.66	1844	1244	1.22	3.23	15.34
8863	11.4	16	2.35	2.65	37.3	1.1	5.82	0.57	4.41
8864	18.4	17	2.17	2.66	707	455	1.25	1.95	8.63
8865	18.8	17.7	2.16	2.66	1002	1020	0.99	2.29	9.90
8866	15.3	13.8	2.26	2.67	107	118	0.95	0.83	4.60

Table 2. Continued

Depth	Helium Porosity	Summation Fluids Porosity	Bulk Density	Grain Density	Nitrogen Permeability		Anisotropy	Reservoir Quality Index	Flow Zone Indicator
					Horizontal	Vertical			
8867	17.8	13.4	2.19	2.66	585	342	1.31	1.80	8.31
8868	19.5	18.6	2.14	2.66	708	565	1.12	1.89	7.81
8869	15.1	19.2	2.28	2.69	225	220	1.01	1.21	6.81
8870	18.4	12.3	2.17	2.66	684	604	1.06	1.91	8.49
8871	17.9	16	2.19	2.67	383	365	1.02	1.45	6.66
8872	19.7	18.7	2.14	2.66	961	811	1.09	2.19	8.94
8873	18.4	15.8	2.18	2.67	679	588	1.07	1.91	8.46
8874	18.5	18.7	2.18	2.67	1500	482	1.76	2.83	12.46
8875	18.2	18.1	2.18	2.66	1080	856	1.12	2.42	10.87
8876	17.8	15.4	2.19	2.66	564	375	1.23	1.77	8.16
8877	18.0	18.5	2.18	2.66	1117	429	1.61	2.47	11.27
8878	17.9	13.8	2.18	2.66	919	635	1.20	2.25	10.32
8879	15.1	16.4	2.26	2.66	1125	598	1.37	2.71	15.24
8880	12.3	15.1	2.33	2.66	154	0.75	14.33	1.11	7.92
8881.5	8.9	8.1	2.44	2.68	0.02	0.01	1.41	0.01	0.15
8891	15.6	14.9	2.27	2.69	1.01	2.45	0.64	0.08	0.43
8892	15.6	12.2	2.26	2.68	0.71	0.45	1.26	0.07	0.36
8893	15.9	10.7	2.25	2.67	1.6	0.61	1.62	0.10	0.53
8894	12.6	9.4	2.33	2.67	1.78	0.47	1.95	0.12	0.82
8895	12.8	10.1	2.33	2.67	3.73	2.63	1.19	0.17	1.15
8896	9.9	9.3	2.45	2.72	0.39	0.05	2.79	0.06	0.57
8897	9.8	8.6	2.45	2.72	0.16	0.1	1.26	0.04	0.37
8898	11.2	8.9	2.37	2.67	0.25	0.06	2.04	0.05	0.37
8899	9.8	6.8	2.61	2.89	0.26	0.04	2.55	0.05	0.47
8900	11.5	8.4	2.35	2.66	0.51	0.06	2.92	0.07	0.51
8901	9.9	9.5	2.40	2.66	0.38	0.08	2.18	0.06	0.56
8904	13.3	11.2	2.31	2.66	1.74	1.66	1.02	0.11	0.74
8905	11.8	12.4	2.39	2.71	3.54	3.1	1.07	0.17	1.29
8906	11.9	10.9	2.35	2.67	0.44	0.08	2.35	0.06	0.45
8907	12.8	10.9	2.32	2.66	5.08	2.28	1.49	0.20	1.35
8908	13.2	13.8	2.32	2.67	1.87	0.59	1.78	0.12	0.78
8909	13	11.4	2.31	2.66	5.55	2.52	1.48	0.21	1.37
8910	13.6	13.3	2.31	2.67	12.3	7.29	1.30	0.30	1.90
8911	10.5	7.5	2.41	2.69	4.06	0.18	4.75	0.20	1.66
8912	11.5	14	2.35	2.66	1.58	0.49	1.80	0.12	0.90
8913	9.6	6.7	2.40	2.66	1.21	0.56	1.47	0.11	1.05
8914	12.1	8.7	2.34	2.66	48.7	33	1.21	0.63	4.58
8915	2.5	6.3	2.58	2.65	0.23	0.03	2.77	0.10	3.71
8916	11.8	11.1	2.36	2.68	18.1	18.1	1.00	0.39	2.91
8917	11.4	9.4	2.39	2.7	76.7	93.2	0.91	0.81	6.33
8918	11.4	7.7	2.38	2.69	642	198	1.80	2.36	18.31
8919	13.2	11.4	2.32	2.67	120	71	1.30	0.95	6.23
8920	15.3	12.9	2.26	2.67	299	85.8	1.87	1.39	7.68
8924	3.3	3.7	3.05	3.15	0.01	0.01	1.00	0.02	0.51
8925	11.3	15.6	2.37	2.67	0.27	0.82	0.57	0.05	0.38
8926	9.4	12.4	2.49	2.75	0.33	0.09	1.91	0.06	0.57
8927	14.1	13.7	2.31	2.69	0.64	0.11	2.41	0.07	0.41
8929	16.6	15.2	2.24	2.68	0.55	0.5	1.05	0.06	0.29
8930	14.2	10.7	2.33	2.71	1.32	0.69	1.38	0.10	0.58
8931	13.1	14.1	2.33	2.68	4.65	1.32	1.88	0.19	1.24
8932	10.8	7.9	2.40	2.69	0.41	0.06	2.61	0.06	0.51
8933	9.6	8.8	2.41	2.67	1.05	0.07	3.87	0.10	0.98
8934	11.3	5.7	2.39	2.69	0.75	0.03	5.00	0.08	0.63
8937	3.6	2.5	2.76	2.86	0.17	0.01	4.12	0.07	1.83
8940	5.6	3	2.68	2.84	1.11	0.26	2.07	0.14	2.36
8941	5.4	6.6	2.58	2.73	0.15	0.03	2.24	0.05	0.92
8942	8.3	8.7	2.46	2.68	0.17	0.09	1.37	0.04	0.50

Table 2. Continued

Depth	Helium Porosity	Summation Fluids Porosity	Bulk Density	Grain Density	Nitrogen Permeability		Anisotropy	Reservoir Quality Index	Flow Zone Indicator
					Horizontal	Vertical			
8944	16.7	11.5	2.22	2.66	2.58	0.52	2.23	0.12	0.62
8945	17.3	12.6	2.20	2.66	0.67	0.51	1.15	0.06	0.30
8946	16.1	14	2.23	2.66	1.62	0.63	1.60	0.10	0.52
8947	16.8	14.8	2.21	2.66	0.34	0.19	1.34	0.04	0.22
8948	16.7	10.7	2.22	2.67	0.41	0.19	1.47	0.05	0.25
8949	14.6	17.9	2.29	2.68	0.13	0.05	1.61	0.03	0.17
8950	9.3	8.4	2.44	2.69	0.7	0.01	8.37	0.09	0.84
8951	10.8	10	2.41	2.7	0.02	0.01	1.41	0.01	0.11
8952	8.3	5.9	2.46	2.68	0.02	0.01	1.41	0.02	0.17
8953	10.4	8.1	2.43	2.71	0.19	0.09	1.45	0.04	0.37
Mean	13.18	12.57	2.33	2.68	181.80	114.06	2.35	0.70	4.04
Min	2.5	2.5	2.13	2.65	0.01	0.01	0.57	0.01	0.11
Max	20.4	22.1	3.05	3.15	1844	1244	38.21	3.23	21.72

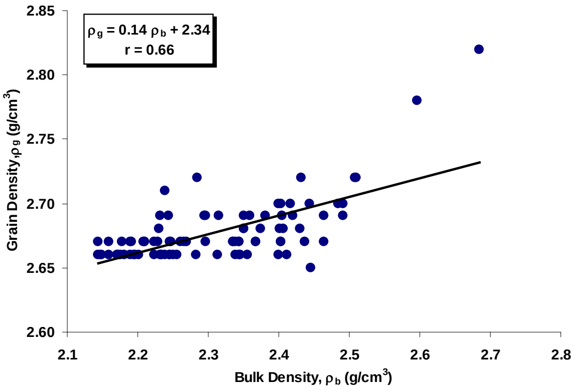

(A)

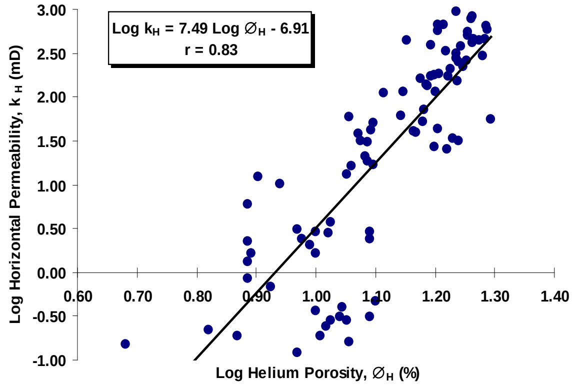

(A)

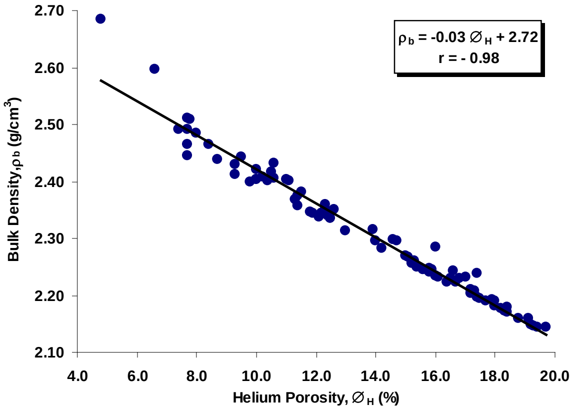

(B)

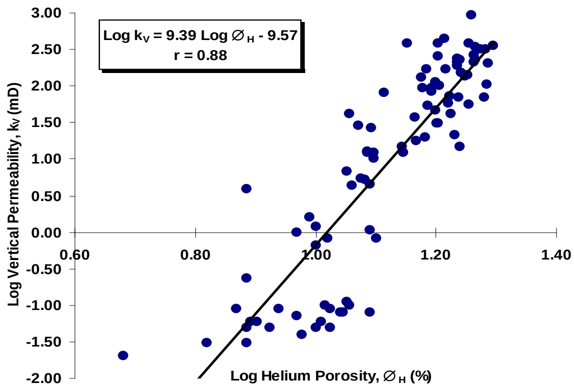

(B)

Fig. (6) Relationships between Bulk Density Values and the Determined Helium Porosity (A), and Grain Density (B) for N. Qarun-1 Samples.

Fig. (7) Plotting of the Helium Porosity ($\varnothing_H$) versus the Vertical and Horizontal Permeabilities for Samples of Well N. Qarun-1.

The calculated regression equations for these relations have the forms:

$\rho g = 0.14\, \rho b + 2.34$, $r = 0.66$ (5)

$\rho b = -0.03\, \varnothing_H + 2.72$, $r = -0.98$ (6)

The horizontal permeability (k_H), on the other hand, was plotted against the helium porosity ($\varnothing_H$) for samples of N. Qarun-1 (Fig. 7A). The horizontal permeability is dependant mainly upon the measured porosity in a very good direct proportional relationship (r = 0.83). On the other side, the measured permeability in the vertical direction (k_V) was plotted against the Helium porosity (Fig. 7B) in a very good linear relationship (r = 0.88). Comparing the correlation coefficients of both relationships indicate a main contribution of permeability from fracture porosity.

The difference in permeability readings in both the vertical and horizontal directions gave rise to anisotropy degree vary from 0.39 to 14.26 (very high anisotropy) of average 2.14 (moderate anisotropy). The anisotropy fraction values (< 1.0) could be attributed to permeability values higher in the vertical direction than that in the horizontal direction, at some depths which ensures the presence of fracture porosity and permeability at these depths. These fracture porosity and permeability led to fair porosity values accompanied with very high permeability values. Presence of very high anisotropy values reach to 14.26 could be attributed to some fissile beds containing high clay content. The calculated regression equations for these relations have the forms:

$\text{Log}\, k_H = 7.49\, \text{Log}\, \varnothing_H - 6.91$, $r = 0.83$ (7)

$\text{Log}\, k_V = 9.39\, \text{Log}\, \varnothing_H - 9.57$, $r = 0.88$ (8)

On the other hand, summation fluids porosity ($\varnothing_S$) was plotted against the permeability in both vertical and horizontal permeability (Fig. 8: A and B) with lower correlation coefficient than that in the case of Helium porosity determination, which could be attributed to the high clay content. So, permeability values could be calculated in terms of helium porosity in a precision degree higher than that in the case of using the summation fluids porosity values.

$\text{Log}\, k_H = 4.47\, \text{Log}\, \varnothing_S - 3.47$, $r = 0.66$ (9)

$\text{Log}\, k_V = 5.77\, \text{Log}\, \varnothing_S - 5.33$, $r = 0.72$ (10)

However, the summation fluids porosity of N. Qarun-1 samples is directly proportional to its helium porosity (Fig. 9) and could be calculated in terms of each other according to the following equation:

$\varnothing_S = 0.90\, \varnothing_H + 0.83$, $r = 0.73$ (11)

Plotting of the porosity values derived from the neutron and density logs against that obtained from the core analysis is one of the main tools used for correcting the well log data through offering an equation relating the interpreted Neutron-Density Porosity ($\varnothing_{N\text{-}D}$) to the helium porosity ($\varnothing_H$).

$\varnothing_{N\text{-}D} = 2.42\, \varnothing_H - 12.51$, $r = 0.56$ (12)

The relatively low correlation coefficient obtained for that equation could be related to the difference in the applied tools, concept and conditions of application. However, this equation is more reliable than that obtained from plotting the summation fluids porosity against the Neutron-Density porosity (r = 0.27).

However, distribution of permeability values is more or less similar in both vertical and horizontal directions. The vertical permeability values have an excellent direct relationship to the horizontal permeability (Fig. 10) and could be calculated in terms of each other according to the following empirical relationship:

$\text{Log}\, k_V = 1.11\, \text{Log}\, k_H - 0.60$, $r = 0.93$ (13)

Regarding N. Qarun-3 samples, the obtained relationships are more or less similar to those of N. Qarun-1 samples but with lower reliability and higher scattering. The bulk density values are mostly dependant on the helium porosity values rather than the dependence on the grain density values, r = - 0.94 & r = 0.69, respectively (Fig. 11); due to a more or less heterogeneity in the mineralogical composition of the studied samples.

$\rho g = 0.27\, \rho b + 2.08$, $r = 0.69$ (14)

$\rho b = -0.03\, \varnothing_H + 2.75$, $r = -0.94$ (15)

The horizontal and vertical permeability (k_H & k_V) were also plotted against the helium porosity ($\varnothing_H$) for samples of N. Qarun-3 (Fig. 12: A and B). Both the horizontal permeability and the vertical permeability are dependant mainly upon the measured helium porosity in a direct proportional relationship, r = 0.66 & 0.68, respectively. Comparing the correlation coefficients of both relationships with those obtained for N. Qarun-1 samples indicate a more heterogeneity for the case of N. Qarun-3 samples.

$\text{Log}\, k_H = 4.55\, \text{Log}\, \varnothing_H - 3.89$, $r = 0.66$ (16)

$\text{Log}\, k_V = 5.07\, \text{Log}\, \varnothing_H - 4.91$, $r = 0.68$ (17)

The difference in permeability readings in both the vertical and horizontal directions gave rise to anisotropy degree vary from 0.57 to 38.2 (very high anisotropy) of average 2.35 (moderate anisotropy).

The anisotropy fraction values (< 1.0) are due to permeability values in the vertical direction higher than that in the horizontal direction at some depths, which reveals the presence of some fractures at these depths. Presence of very high anisotropy values reaching to 38.2 could be attributed to some fissile beds containing higher clay content than the case of N. Qarun-1 samples.

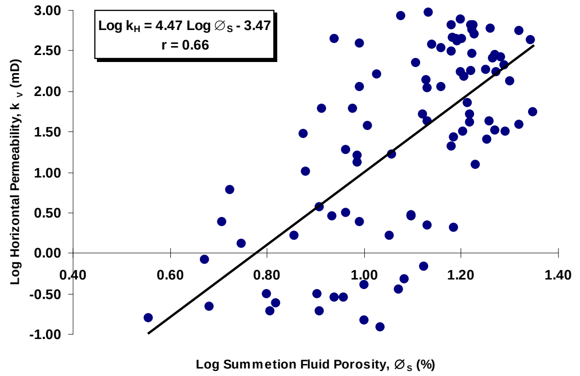

(A)

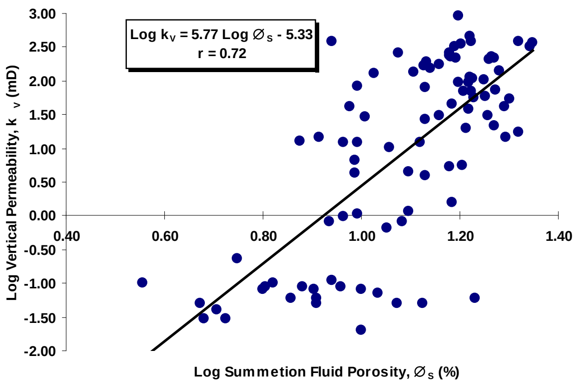

(B)

Fig. (8) Plotting of the Summation Fluid Porosity ($\varnothing_S$) versus the Vertical and Horizontal Permeabilities for samples of Well N. Qarun-1.

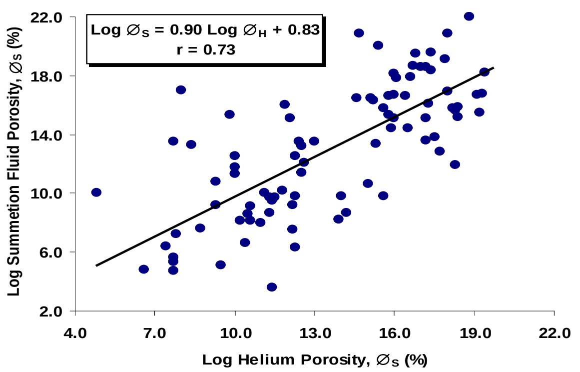

Fig. (9) Plotting of the Determined Helium Porosity ($\varnothing_H$) Versus the Summation Fluids Porosity ($\varnothing_S$) for Samples from Well N. Qarun-1.

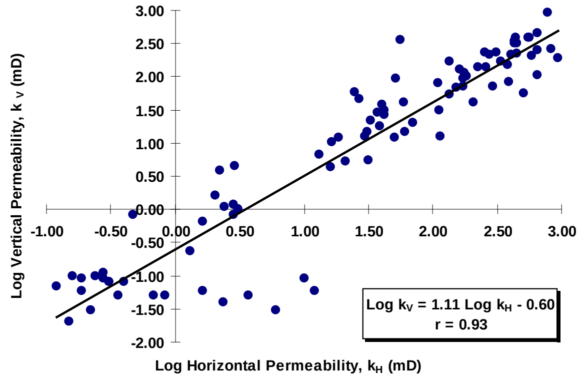

Fig. (10) A Plot of the Measured Vertical Permeability (k_V) Versus the Horizontal Permeability (k_H) for Samples From Well N. Qarun-1.

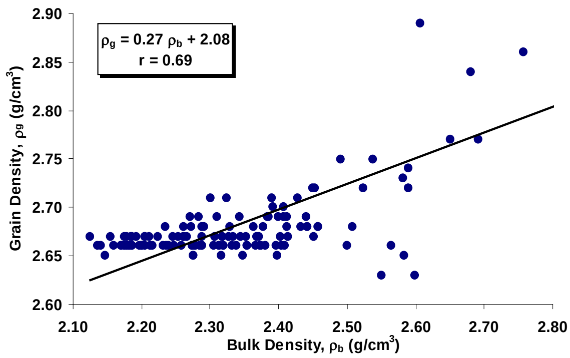

(A)

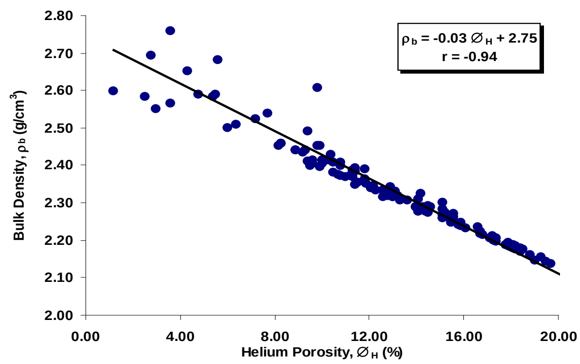

(B)

Fig. (11) Bulk Density Values (ρ_b) for N. Qarun-3 Samples in Relation to: (A) Grain Density Values (ρ_g), and (B) Helium Porosity, $\varnothing_H$.

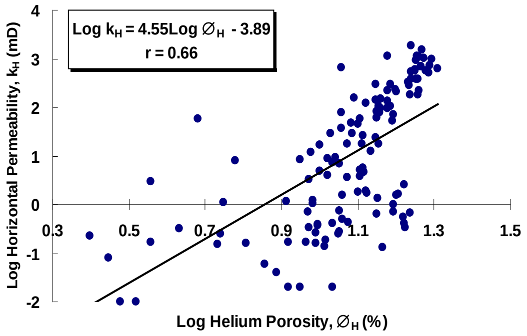

(A)

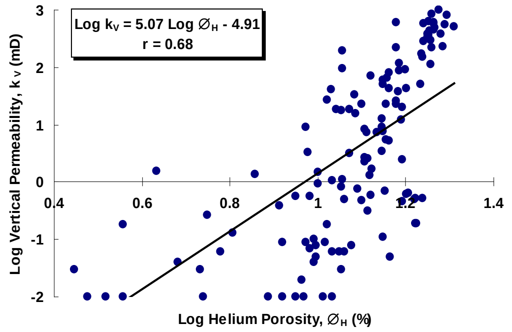

(B)

Fig. (12) Plotting of the Helium Porosity ($\varnothing_H$) versus: A) Horizontal Permeability, and B) Vertical Permeability for samples of Well N. Qarun-3.

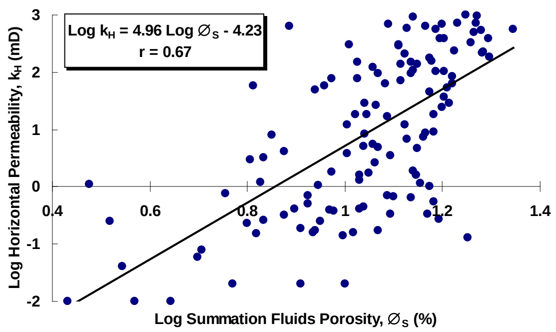

(A)

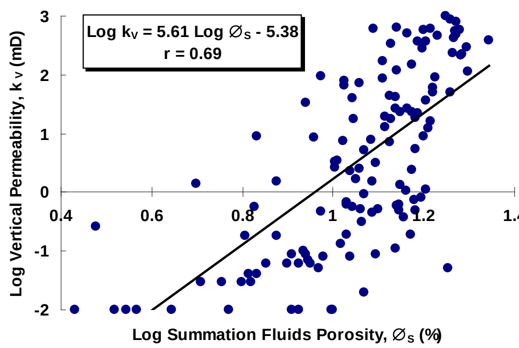

(B)

Fig. (13) Plotting of the Summation Fluids Porosity versus: A) Horizontal Permeability, and B) Vertical Permeability for Samples from Well N. Qarun-3.

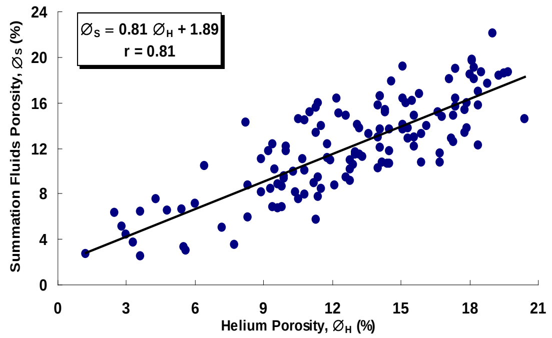

Fig. (14) A Plot of the Helium Porosity versus the Summation Fluids Porosity for Samples from Well N. Qarun-3.

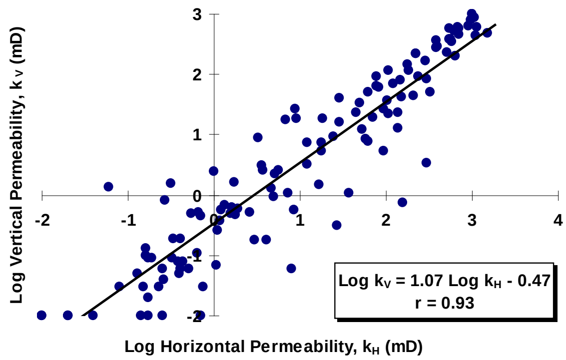

Fig. (15) A Plot of the Measured Vertical Permeability versus the Horizontal Permeability for Samples from Well N. Qarun-3.

On the other hand, the vertical and horizontal permeability were also plotted against the summation fluids porosity ($\varnothing_S$) (Fig. 13: A and B) with relatively low correlation coefficients, which could be attributed to the high clay content.

So, like the case of N. Qarun-1 samples, permeability is recommended to be calculated in terms of helium porosity in a precision degree higher than obtained using the summation fluids porosity values.

$$\text{Log } k_H = 4.96 \text{ Log } \varnothing_S - 4.23 \quad , r = 0.67 \qquad (18)$$

$$\text{Log } k_V = 5.61 \text{ Log } \varnothing_S - 5.38 \quad , r = 0.69 \qquad (19)$$

The summation fluids porosity of N. Qarun-3 samples is directly proportional related to its helium porosity in relatively high precision degree (Fig. 14) and could be calculated in terms of each other according to the following equation:

$$\varnothing_S = 0.81 \varnothing_H + 1.89 \quad , r = 0.81 \qquad (20)$$

The comparison of the two equations obtained for the N. Qarun-1 and N. Qarun-3 cases, indicates that, the helium porosity values are to be multiplied by a factor to obtain the summation fluids porosity, i.e. the helium porosity in both cases is less than the summation fluids porosity. This could be attributed to presence of some clay content.

Dislike the case of N. Qarun-1, the plotting the porosity values derived from the neutron and density logs against those obtained from the summation fluids and helium tools gave rise to unreliable equation (r = 0.20 and 0.23, respectively) and could not be applied to further well logging corrections.

So, it is hardly recommended to apply that equation obtained for N. Qarun-1 samples for the corrections of the logging through the other 7 wells including N. Qarun-3.

Similarity between the distribution of permeability values measured in the horizontal and vertical direction is noticed for samples from N. Qarun-3 (Fig. 15). Therefore, the vertical permeability values could be calculated in terms of the horizontal permeability with a very high precision according to the following empirical relationship:

$$\text{Log } k_V = 1.07 \text{ Log } k_H - 0.47 \quad , r = 0.93 \qquad (21)$$

RESERVOIR ZONATION

In the present study and based on the obtained data from the X-Y plot of reservoir properties, it is preferred to use the helium porosity and the horizontal permeability values (both parameters gave high reliability relationships and less scattering data) for the reservoir zonation and the reservoir quality discrimination.

To achieve the reservoir zonation, a porosity cutoff value equals 10 %, permeability value equals 1 md, anisotropy value equals 2, and continuity of the horizon for more than 5 feet have been taken as reservoir parameters cutoffs for both the N. Qarun-1 and N. Qarun-3 wells. Matching the data of the routine core analysis of the lower part of Bahariya Formation in well N. Qarun-1 and their vertical tracing through the given depths (Fig. 16) indicates acceptable storage capacity parameters only through depths between 8897" and 8967" out of the total cored depth.

Helium porosity values in this range are high (7.70-19.70 % of average 15.28 %), and the permeability values are also high (0.84-937 md of average 228.7 md).

The bulk density values of the discriminated zone are low (2.14-2.51 g/cm^3 of average 2.26 g/cm^3) and characterized also by low anisotropy values (0.39-4.10 of average 1.5).

The anisotropy for the other horizons may reach up to 14 giving rise to a high heterogeneity in the storage capacity distribution in the 3-D, which could be attributed to the heterogeneous effect of the diagenetic factors through the studied depth interval.

Some anisotropy anomalies at different depths, e.g. 8881", 8893", and 8968" are reasonably accompanied with gabs between the vertical and horizontal permeability values, and with anomalies in the vertical distribution of the porosity and bulk density at the same depths (Fig. 16). These anomalies, however, are recommended to be used as a marker anomaly or trace to follow up the reservoir horizon in the different bore holes.

The N. Qarun-3, analysis of the routine core data of also the lower part of Bahariya Formation and its vertical tracing through the given depths (Fig. 18) indicates acceptable storage capacity parameters through a main depth interval 8825"-8880", and two subsidiary depth intervals, 8788"-8803", and 8914"-8920" with some thin horizons having bad storage capacity properties intercalated through these intervals.

The anisotropy for some horizons are very high forming anomalous peaks, may reach up to 35 at depths 8802", 8828", 8856", 8880", 8937", and 8950" giving rise to a high level of heterogeneity in the storage capacity distribution in the 3-D, which could be attributed to the heterogeneous effect of the diagenetic factors through the studied depth interval. Like the case of the N. Qarun-1 samples, three anomalous anisotropy intervals are accompanied with gab between the permeability values in the vertical and horizontal directions, and with anomalies in the vertical distribution of the porosity and bulk density at the same depths (Fig. 17). Therefore, these anomalies are highly recommended to be used as marker anomalies or traces to follow up the reservoir horizon in the different bore holes in N. Qarun oil field.

In general, the cored zones in N. Qarun-3 oil well seem to have better reservoir characteristics than that of the cored depths in N. Qarun-1 but with higher anisotropy and heterogeneity.

RESERVOIR QUALITY DISCRIMINATION

In the present study, the reservoir quality index (RQI) of the technique of Amaefule et al. (1993) was used for the identification of super quality reservoir zones based on high quality values of RQI and FZI. The (RQI) values of the studied samples vary from 0.02 to 2.32 μm of average 0.74 μm, whereas values of the flow zone indictor (FZI) vary from 0.11 to 11.16 μm of average 4.03 μm for well N. Qarun-1. On the other side, (RQI) of well N. Qarun-3 varies from 0.01 to 3.23 μm of average 0.66 μm, whereas the

(FZI) values vary from 0.11 to 21.72 μm of average 3.89 μm.

The standard deviations of the calculated (RQI) and the flow zone indicator (FZI) data are higher for samples from well N. Qarun-3 (0.85 and 4.67, respectively) than that for samples of Well N. Qarun-1 (0.65 and 3.01, respectively), i.e. the calculated data for N. Qarun-1 is more homogeneity than that of N. Qarun-3. Figures 16 and 17 show how RQI and FZI were selected for dividing the reservoir interval into different zones.

Achieving the best reservoir quality discrimination, permeability value equals 100 md, RQI equals 1 μm and for FZI equals 5 μm have been taken as reservoir parameters cutoffs for both the N. Qarun-1 and N. Qarun-3 wells. Taking into consideration the reservoir cutoff values and the continuity for the highest values for more than 5 feet depth interval, two super quality zones were recognized for well N. Qarun-1 at depth intervals 8944-8957" and 8960-8967".

These two zones have permeability values vary from 173 to 937 md of average 441.5 md, (RQI) vary from 1.01 to 2.32 μm of average 1.53 μm and have (FZI) values vary from 5.04 to 11.16 μm of average 7.24 μm. On the other side, the N. Qarun-3 well has only one thick super quality zone in the depth interval 8867-8880". This distinct zone has permeability values vary from 154 to 1500 md of average 763.1 md, (RQI) values vary from 1.11 to 2.83 μm of average 2.00 μm and have (FZI) values vary from 6.66 to 15.24 μm of average 9.41 μm.

Comparing the (RQI) and (FZI) parameters for the super quality zones in both wells indicates higher reservoir quality for the super quality zones in well N. Qarun-1 than that for well N. Qarun-3.

Figure 18 matches plotting of the reservoir quality index (RQI) of well N. Qarun-1 versus bulk density, porosity and permeability. It shows that (RQI) of the studied samples could be calculated in terms of these parameters in a binomial equation for the (RQI) - ρ_b relation and exponential equations for the (RQI) - $\varnothing$ and (RQI) – k relations. It is declared that, using the $\varnothing_H$ and k_H data for calculating the (RQI) is more reliable than using $\varnothing_S$ and k_V (Fig 18: B and C).

On the other hand, plotting the (FZI) values of the same well versus the same parameters shows that the (FZI) could be calculated in terms of these parameters, like the case of the (RQI) relations, in a binomial equation for the (RQI) - ρ_b relation and exponential equations for the (FZI) - $\varnothing$ and (FZI) – k relations. It is deduced also that, using the helium porosity and the horizontal permeability data for calculating the (FZI) is more reliable than using the summation fluids porosity and the vertical permeability (Fig. 19).

A comparison between the correlation coefficient of the different parameters' relationships with the (RQI) and (FZI) indicates a higher reliability for the relations with the (RQI). These figures show also that, both the (RQI) and the (FZI) values are mainly contributed by the permeability values ($0.84 < r < 0.997$) rather than the porosity values ($0.56 < r < 0.79$).

Like the case of well N. Qarun-1, the bulk density, porosity and permeability values of the N. Qarun-3 were plotted against the (RQI) and the (FZI) values (Figs. 20 and 21). Both figures show a dependence of both the reservoir quality parameters on the bulk density (binomial relation), on porosity and permeability values (both in exponential relations).

A preferring for using the Helium porosity and the horizontal permeability in calculating both the (RQI) and the (FZI) is declared with higher reliability than using the summation fluids porosity and the vertical permeability values.

From the statistical processing of the valid petrophysical data in the present study, a number of empirical equations are introduced in figures 18-21 to be used for calculating both the (RQI) and (FZI) quality values in terms of the valid bulk density data, both measured helium and summation fluids porosity data and both vertical and horizontal permeability.

From the statistical processing of the whole data, it is recommended to use the valid permeability data to calculate the (RQI) and (FZI) values for the other wells in the field and to predict the permeability values in both the vertical and horizontal directions in terms of the quality control parameters of the field ($0.814 < r < 0.994$). It could be also extended for further activities at the borders of the field.

Using the porosity and bulk density values for calculating the quality control parameters, are recommended to be used in a limited scale to calculate the quality control parameters for each well ($0.32 < r < 0.57$ & $0.516 < r < 0.739$, respectively) and to use the quality control parameters of each well to predict the missed density and porosity data within the same well.

*** RQI – bulk density relationship:**

$$RQI = 7.8\ \rho_b^2 - 41.3\,\rho_b + 54.3 \quad , r = -0.739 \quad (22)$$

*** RQI – permeability relationships:**

$$RQI = 0.098\ k_H^{\ 0.46} \quad , r = 0.994 \quad (23)$$

$$RQI = 0.180\ k_V^{\ 0.38} \quad , r = 0.914 \quad (24)$$

*** FZI – permeability relationships:**

$FZI = 0.852\ k_H^{\ 0.37}$, r = 0.928 (25)

$FZI = 1.419\ k_V^{\ 0.29}$, r = 0.812 (26)

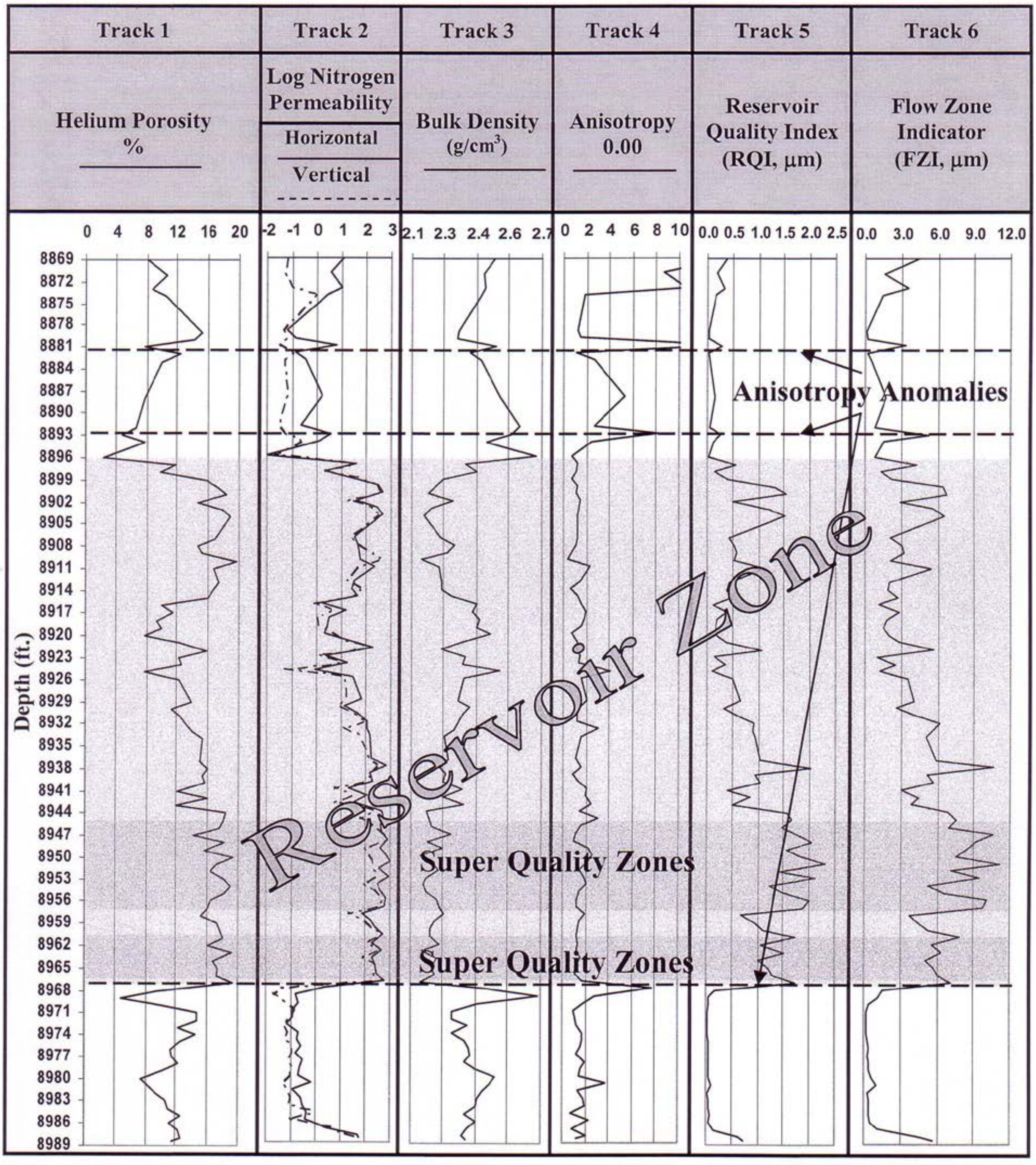

Fig. (16) Vertical Tracing of the Storage Capacity Properties, RQI, FZI and Anisotropy of the Lower Part of Bahariya Formation in N. Qarun-1 Oil Well.

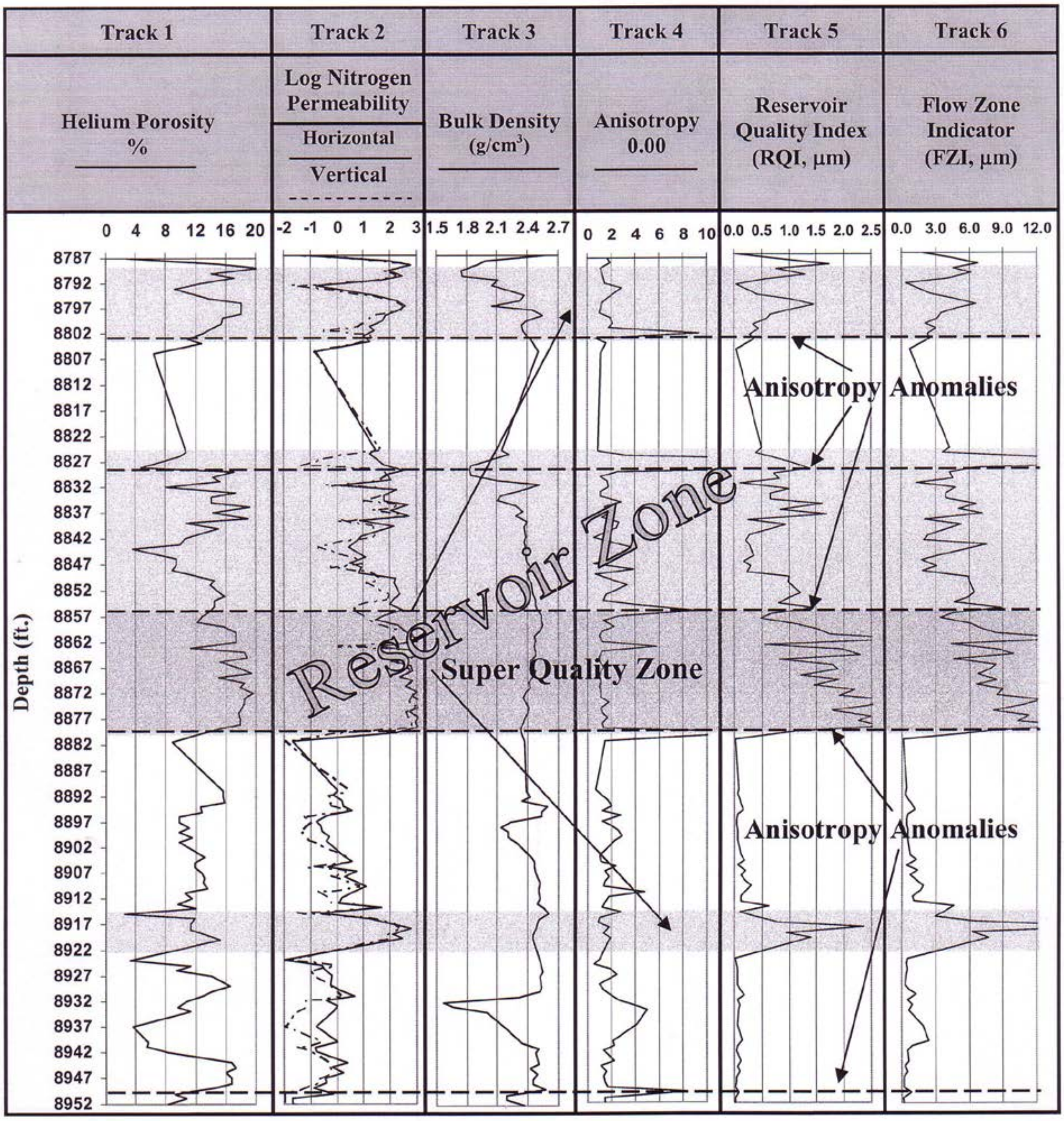

Fig. (17) Vertical Tracing of the Storage Capacity Properties, RQI, FZI and Anisotropy of the Lower Part of Bahariya Formation in N. Qarun-3 Oil Well.

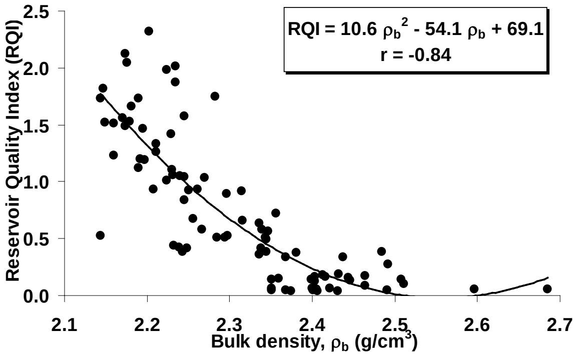

(A)

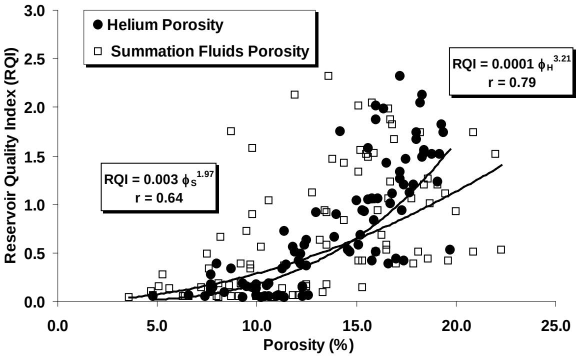

(B)

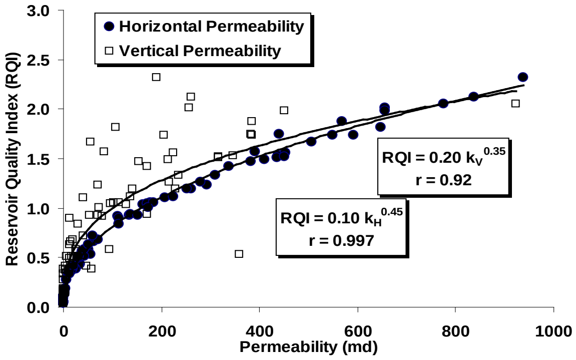

(C)

Fig. (18) Plotting of the Reservoir Quality Index (RQI) versus; A) bulk density (ρ_b), B) Helium and summation fluids porosity (($\varnothing_H$ & $\varnothing_S$), and C) horizontal and vertical Permeability (k_H & k_V) for samples of Well N. Qarun-1.

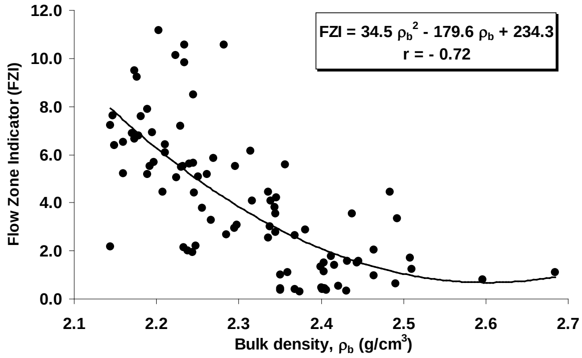

(A)

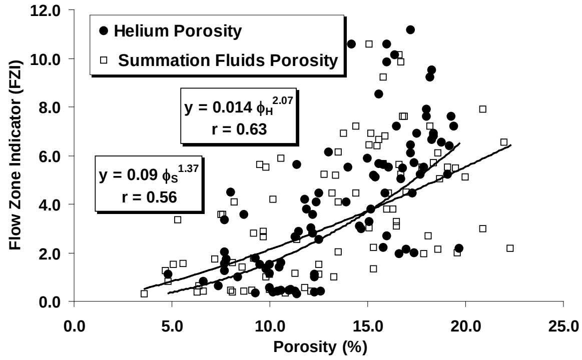

(B)

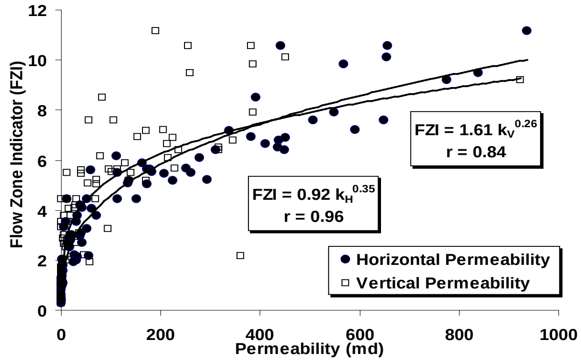

(C)

Fig. (19) Plotting of the Flow Zone Indicator (FZI) versus; A) bulk density (ρ_b), B) Helium and summation fluids porosity (($\varnothing_H$ & $\varnothing_S$), and C) horizontal and vertical Permeability (k_H & k_V) for Samples of Well N. Qarun-1.

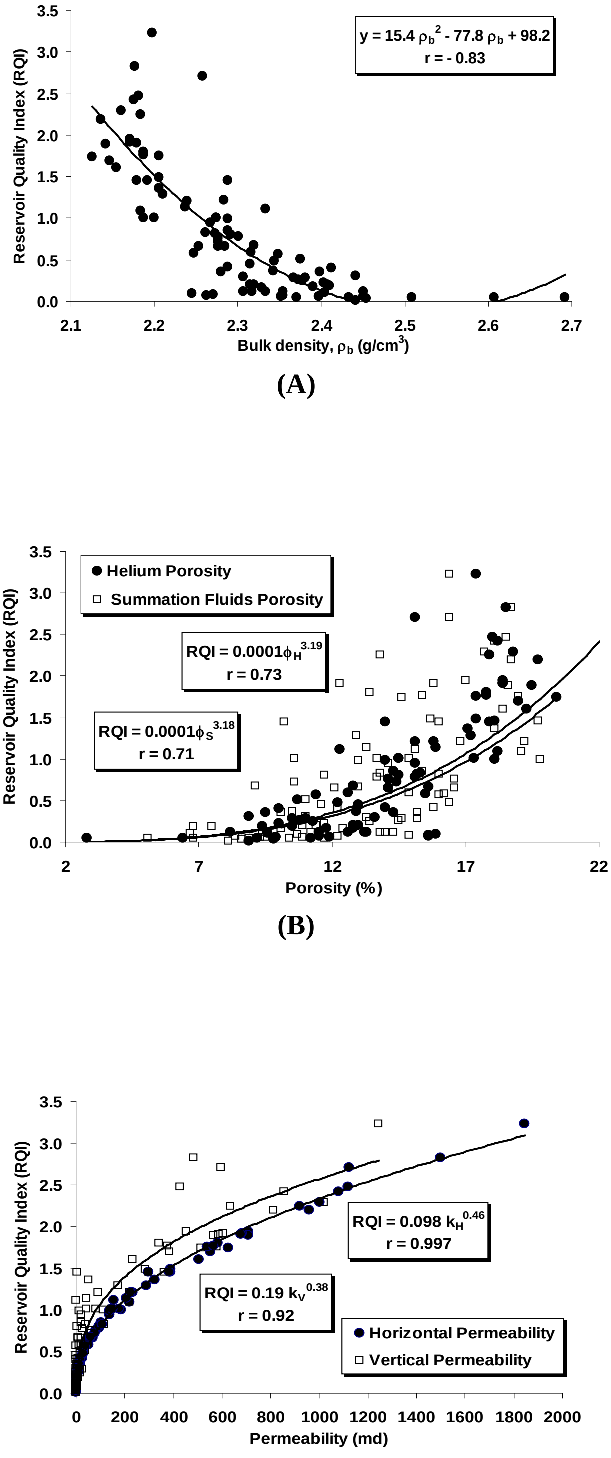

Fig. (20) Plotting of the Reservoir Quality Index (RQI) versus; A) bulk density (ρ_b), B) Helium and summation fluids porosity ($\varnothing_H$ & $\varnothing_S$), and C) horizontal and vertical Permeability (k_H & k_V) for samples of Well N. Qarun-3.

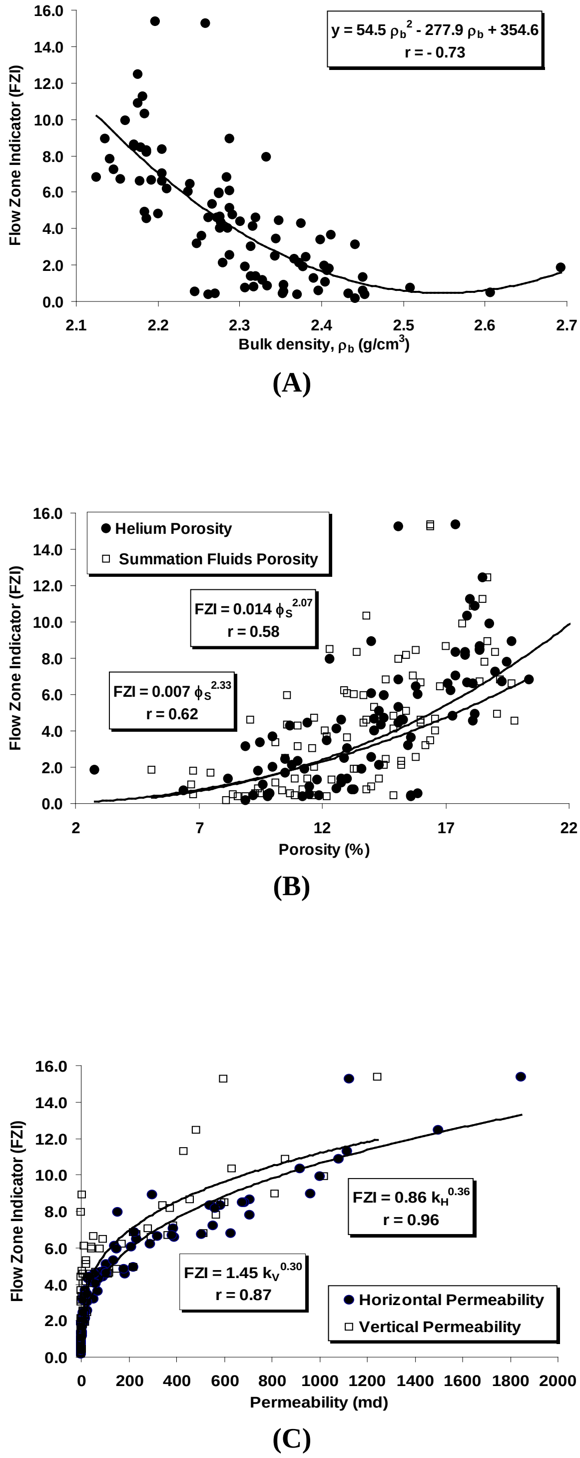

Fig. (21) Plotting of the Flow Zone Indicator (FZI) versus; A) bulk density (ρ_b), B) Helium and summation fluids porosity (($\varnothing_H$ & $\varnothing_S$), and C) horizontal and vertical permeability (k_H & k_V) for samples of Well N. Qarun-3.

CONCLUSIONS

The helium porosity values for the studied sandstones of the lower part of Bahariya Formation in N. Qarun Oil Field show a main contribution to both of the bulk density values and the horizontal permeability (k_H) in high reliable proportional relationships.

Permeability values could be calculated in terms of helium porosity in a higher precision level than that in terms of the summation fluids porosity.

The anisotropy of permeability (k_H/k_V) for the studied samples indicates increasing the heterogeneity to the south in the center of the field at well N. Qarun-3. The presence of some anisotropy fraction values (< 1.0) indicates higher permeability in the vertical direction, i.e. fracture porosity and permeability.

Matching the data of the lower part of Bahariya Formation and its vertical tracing through the given depths indicates acceptable storage capacity parameters at most of the middle parts in the North Qarun Oil Field.

The anisotropy anomalies in permeability are recommended to be used as a marker anomaly or trace to follow up the reservoir horizon in the different bore holes.

Usage of Amaefule et al. parameters (1993) allowed discrimination of two super permeability zones for well N. Qarun-1 and only one thick super permeability zone in well N. Qarun-3.

Comparing the (RQI) and (FZI) parameters for the super quality zones in both wells indicates higher reservoir quality for the super quality zones in well N. Qarun-1 at the borders of the field than that for well N. Qarun-3 in the center of the field.

ACKNOWLEDGMENT

The authors would like to acknowledge Qarun Oil Company for release the applied data and the license for data processing and interpretation. The authors are praying to ALLAH (SWAT) by summoning to be merciful toward the spirits of both Prof. Mohamed A. Ragab and Prof. Mahomoud A. El-Hefnawy for their support at the beginning of the present study.

REFERENCES

Abd El Aal, A., 1990. Subsurface study of the Abu Gharadig Basin, Western Desert, Egypt. M.Sc. Thesis, Ain Shams Univ., 150 p.

Abd El Aal, A. and Moustafa, A.R., 1988. Structural framework of the Abu Gharadig basin, Western Desert, Egypt. 9th EGPC Exploration & Production conference, 16 p.

Abd El-Aziz, M., Moustafa, A.R. and Said, S.E., 1998. Impact of basin inversion on hydrocarbon habitat in the Qarun concession, Western Desert, Egypt. proceedings of the 14th Petroleum Exploration and Development conference, Cairo, E.G.P.C., vol. 1, pp.139-155.

Abdalla, A.Y. and El-Bassyouni, A.A., 1985. Primary sedimentary structures and sedimentary environments of the Bahariya Formation "Lower Cenomanian", Bahariya Oasis, Egypt. Ann. Geol. Surv. Egypt, vol. xv, pp. 267-274.

Al-Dhafeeri, A.M. and Nasr-El-Din, H.A., 2007. Characteristics of high-permeability zones using core analysis, and production logging data. J. Petrol. Sci. and Eng., vol. 55, pp. 18–36.

Amaefule, J.O., Altunbay, M., Tiab, D., Kersey, D.G., Keelan, D.K., 1993. Enhanced reservoir description: using core and log data to identify hydraulic (flow) units and predict permeability in uncored intervals/wells. SPE 26436. Presented at the Annual Technical Conference and Exhibition, Houston, TX, pp. 3–6. October.

Barakat, M.G. and Darwish, M., 1987. Stratigraphy of the Lower Cretaceous sequence in Mersa Matruh area, north Western Desert, Egypt. M.E.R.C., Ain Shams Univ., Earth Sci. Series, vol. 1, pp. 48-66.

El Gezeery, M.N., Mohsen, S.M. and Farid, M., 1972. Sedimentary basins of Egypt and their petroleum prospects. 8th Arab Petroleum Congr., Algeris, pp. 15-29.

El-Sayed, A.M.A., Kassab, M.A., El-Safori, Y.A. and Abass, A.E., 2005. Carbonate facies and its reservoir properties, West Tushka, South Western Desert, Egypt. 1st Int. Conf. of the Geology of the Tethys, pp. 267-278.

El Shaarawy, O.A., 1994. Zonation of the Bahariya Formation and Alamein Dolomite Reservoirs in the Razzak oil field, North Western Desert of Egypt. Second international conference on the geology of the Arab world, Cairo University, Cairo, pp. 1-16.

Hanter, G., 1990. The north Western Desert, Egypt; In: The Geology of Egypt. R. Said, Ed., pp. 293-320.

Ibrahim, M.I.A., 2002. Late Albian–Middle Cenomanian palynofacies and palynostratigraphy, Abu Gharadig-5 well, Western Desert, Egypt. J. Cretaceous Research, vol. 23, Issue 6, pp. 775-788.

Khairy, A. and Said, S., 1996. Geological studies on the north Qarun field. Qarun petroleum Co., Internal report, pp.1-8.

Kostandi, A.B., 1959. Facies maps for the study of the Paleozoic and Mesozoic sedimentary basins of

Egyptian region. 1st Arab. Cong., Cairo, paper no. 2, pp. 53-62.

Lüning, S., Kolonic, S., Belhadj, E. M., Belhadj, Z., Cota, L., Bari, G. and Wagner, T., 2004. Integrated depositional model for the Cenomanian–Turonian organic-rich strata in North Africa. J. Earth-Science Reviews, vol. 64, no. 1-2, pp. 51-117.

Said, R., 1962. Geology of Egypt. Elsevier Pub. Co., Amsterdam,, New York, pp. 218-287.

Schlumberger, 1984. Well Evaluation Conference of Egypt. Schlumberger Middle East Service, 64p.

Schlumberger, 1995. Well Evaluation Conference of Egypt. Technical Editing Services, Chester, 87p.

Tammam, M.T., 1996. Basin modeling of Qarun and West Qarun area and its implication on hydrocarbon generation, Western Desert, Egypt; Proc. 13th EGPC petroleum conference, vol. 2, pp. 433-446.

Tiab, D. and Donaldson, E.C., 1996. Petrophysics, Theory and practice of measuring reservoir rock and fluid transport properties. Gulf Publ. Co., Houston, Texas, pp. 205-220.